Estimating the airflow resistivity of porous materials in an impedance tube using an electroacoustic technique

Juan C. Rodríguez[b], Jesús Alba[b], Jorge P. Arenas[a,*], Romina del Rey[b]

[a]*Institute of Acoustics, Univ. Austral of Chile, PO Box 567, 5090000, Valdivia, Chile*
[b]*Universitat Politècnica de València, Campus de Gandia, C/Paraninfo 1, 46730 Grao de Gandia, Valencia, Spain*

Abstract

Airflow resistivity is an essential parameter for characterizing air-saturated porous sound-absorbing materials theoretically and selecting sound-absorbing materials in practice. Although standardized methods can determine this non-acoustic parameter in the laboratory, many indirect alternative methods have been proposed to measure it. One of them is the technique presented in the 1980s by Ingard and Dear using a standing wave tube, a loudspeaker, and two microphones. This paper suggests an electroacoustic procedure based on a modification of the Ingard and Dear setup. Equations are derived through the transfer matrix method. After a simple calibration, the airflow resistivity of a material sample is indirectly estimated from the total electric impedance measured at the loudspeaker input connection terminals. Thus, implementing the proposed method is straightforward and inexpensive, since microphones and complex instrumentation are unnecessary. The method is tested by comparing measured values of the airflow resistivity of different material samples with those obtained through the Ingar and Dear approach and the ISO standardized method. Reasonably good agreement is observed, confirming the validity of the electroacoustic method.

Keywords: airflow resistivity, porous materials, electroacoustics, impedance

tube

1. Introduction

Since airflow resistivity is related to air permeability through porous materials, it is one of the main non-acoustic parameters used to characterize a porous material's sound absorption properties. Several equivalent fluid theoretical models for porous materials with rigid frames use this property [1–5]. Airflow resistance is the ratio of the pressure differential across a material specimen to the normal volumetric air flow through it [1]. Airflow resistivity is defined as the airflow resistance per unit of material thickness. Because this property is directly related to the acoustic energy absorption of a porous material, airflow resistivity is also used for selecting sound-absorbing materials for diverse acoustical applications.

Some authors prefer to use static permeability, which has the dimension of a surface (m^2). Static permeability is defined as the ratio of the dynamic viscosity of air ($\eta \approx 1.84\times10^5$ Ns/m^2 at ambient temperature and pressure conditions) over the static airflow resistivity. Thus, air permeability decreases with increasing airflow resistivity. When compared to resistivity, permeability is independent of the fluid's characteristics.

Both ISO and ASTM have described standardized procedures for measuring airflow resistivity [6–8]. The methods explained in ISO 9053-1 and ASTM C522-03 require a steady airflow passing through a material sample. The pressure drop across the material under study can then be accurately measured. Another method in which the airflow is alternated has been described in the more

*Corresponding author, Tel.: +56-63-2221012
Email address: jparenas@uach.cl (Jorge P. Arenas)

recent ISO 9053-2. In this case, the alternate component of the pressure produced by an oscillating piston in a volume occupied by the test specimen must be measured. Nevertheless, implementing these standardized procedures requires rather complex and special instrumentation, and it is necessary to measure sound pressures at a frequency below the audible range. In addition, pressure differential measurement at particularly low airflow velocities is essential to avoid turbulent flow effects in the material's pores. These experimental complexities have led many researchers to suggest complementary techniques to measure airflow resistivity [9–18].

Reference [19] presented a discussion and a comparison between the results of experiments using the ISO standard and those of experiments using the alternative methods developed by Ingard and Dear [10] and Dragonetti et al. [17].

Garai and Pompoli [20] analyzed the results of an interlaboratory test of airflow resistivity measured according to the ISO standard in ten European laboratories. In one case, they employed an acoustic method not described in the standard [9]. Their study proposed amendments to the ISO standard to improve reproducibility between laboratories. They also confirmed that the acoustic method provides repeatable and acceptable results compared to the standardized procedure.

Two approaches to obtaining airflow resistivity from measurements carried out in impedance tubes were compared by Woodcock and Hodgson [11]. The researchers measured the surface acoustic impedance of a fibrous material according to the two-cavity and the two-thickness methods. They then used their results to determine the material's propagation constant and characteristic impedance. They obtained effective airflow resistivity by combining these results with the Delany and Bazley's empirical power-law relationships [21].

In a method described by Tao et al. [22], the airflow resistivity of a material sample is determined indirectly from the measurement of its surface impedance in two conditions in a traditional impedance tube having a perfectly reflecting end. The transfer functions between the two microphones are measured by placing the test sample with and without a well-defined backing air cavity. Thus, the propagation constant and the characteristic impedance of the material under test are obtained. Finally, the airflow resistivity is determined at a sufficiently low frequency, assuming that the thickness of the sample is small compared to the wavelength.

The use of a three-microphone impedance tube setup for measuring the properties of a porous material, regarded as a fluid equivalent, was reported by Doutres et al. [23]. The technique was used first to determine the material's acoustic properties, and later, non-acoustic properties, including the airflow resistivity in the low-frequency range, were indirectly determined.

The experimental setup for measuring the flow impedance presented by Ingard and Dear [10] is essential for the electroacoustic method proposed in this paper. Their design comprises two measuring microphones and a cylindrical standing wave tube closed with a loudspeaker and a hard reflecting surface at the opposite end. A material sample is placed at a fixed location along the tube, and the complex ratio of the sound pressures is measured at two strategic positions inside the tube. Ingard and Dear theoretically showed that the airflow resistance could be obtained from the imaginary part of the sound pressure complex ratio. From a practical point of view, this approach is straightforward to implement and does not present the low-frequency limitation of the ISO alternated flow method. The method was explored further by Ren and Jacobsen [12] for measuring the dynamic flow impedance of porous materials.

The following sections of this paper present a simple method for measuring the airflow resistivity of a material. This parameter is indirectly estimated in the Ingard and Dear tube from the electric impedance measured at the loudspeaker terminals. Thus, the technique does not require measuring microphones. The authors of this paper have presented a similar approach [18], but applied it to the device proposed by Dragonetti et al. [17]. Preliminary results of this approach were also reported in a congress [24].

This paper is organized as follows. The theoretical details of the proposed approach are detailed in Section 2, while the experimental setup and the materials used to test the method are described in Section 3. The experimental results are reported in Section 4. Finally, Section 5 summarizes the main conclusions.

2. Theory

2.1. The Ingard and Dear acoustic method

In 1985, Ingard and Dear described an alternative method for measuring a porous material's airflow resistance and reactance [10]. Their approach is based on measuring the sound pressure using two microphones placed at two points inside a cylindrical tube with rigid walls and a perfectly rigid termination. The tube's opposite end is closed by an electrodynamic loudspeaker, which acts as a sound source of plane waves. The researchers' experimental arrangement is shown schematically in Figure 1a.

A sample of the porous material under test, with thickness d, is inserted at a distance L_1 from the loudspeaker. L_2 is the distance between the backside of the material (denoted as position 2 in Fig. 1a) and the rigid termination (position 3). One microphone is placed in front of the porous material (indicated as position 1 in Fig. 1a). The second microphone is located in front of the rigid termination.

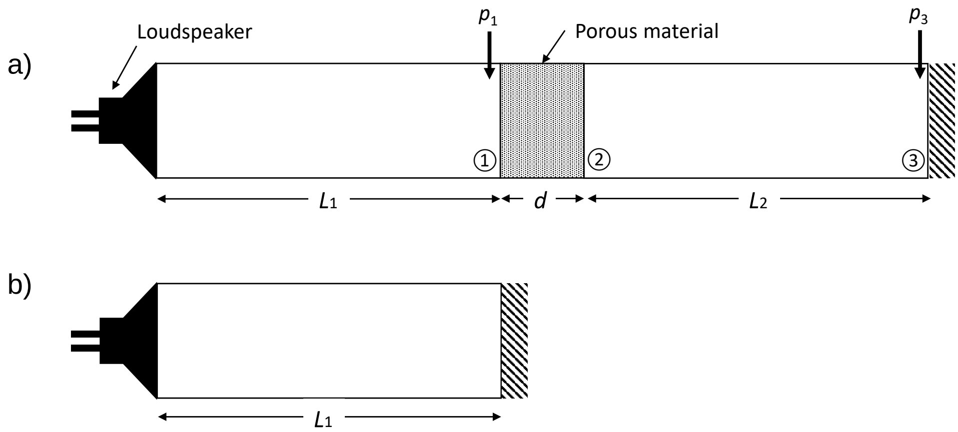

Figure 1: a) Ingard and Dear's experimental arrangement for the measurement of the airflow resistance of a porous material; b) experimental setup used to calibrate the electroacoustic method.

An audio signal generator connected to an amplifier is fed to the loudspeaker to produce a low-frequency sinusoidal sound, so that the microphones measure the resulting sound pressures at positions 1 (p_1) and 3 (p_3). The sound frequency is chosen so that L_2 is an odd number of quarter wavelengths, i.e., $f_n = \frac{(2n-1)c_0}{4L_2}$, where $n = 1, 2, \ldots$ and c_0 is the speed of sound inside the tube. If the tube diameter is D and λ is the wavelength, condition $\lambda \gg 1.7D$ ensures that only plane waves are propagated inside the tube.

Considering that losses inside the tube and material's airflow reactance are negligible at low frequencies, the specific airflow resistance, R_s, can be determined as

$$R_s = \rho_0 c_0 10^{(L_{p1} - L_{p3})/20}, \quad (1)$$

where ρ_0 is the air mean density in the tube and L_{p_1} and L_{p_3} are the sound pressure levels corresponding to p_1 and p_3, respectively. In Eq. (1), it is assumed that the microphones are carefully calibrated to have the same sensitivity and phase.

The system can be described in the low-frequency regime by the transfer matrix method from inspection of Fig. 1a, as

$$\begin{pmatrix} p_1 \\ U_1 \end{pmatrix} = \begin{pmatrix} 1 & Z_A \\ 0 & 1 \end{pmatrix} \begin{pmatrix} \cos(k_0 L_2) & jZ_0 \sin(k_0 L_2) \\ j\sin(k_0 L_2)/Z_0 & \cos(k_0 L_2) \end{pmatrix} \begin{pmatrix} p_3 \\ U_3 \end{pmatrix}, \tag{2}$$

where $k_0 = \omega/c_0$ is the wavenumber in the air; j is the imaginary unit; U_1 and U_3 are the volume velocities at points 1 and 3, respectively; Z_A is the acoustic impedance of the porous material, and $Z_0 = \rho_0 c_0/S$ is the acoustic impedance of air, where S is the cross-sectional area of the tube. It is noted that the reduced transfer matrix in Eq. (2) is valid when $k_c d << 1$, where d is the material thickness and k_c is the characteristic wavenumber of the porous material.

Since the acoustic impedance at the rigid end is infinite ($U_3 = 0$), Eq. (2) becomes

$$\begin{pmatrix} p_1 \\ U_1 \end{pmatrix} = \begin{pmatrix} \cos(k_0 L_2) + \frac{jZ_A \sin(k_0 L_2)}{Z_0} & jZ_0 \sin(k_0 L_2) + Z_A \cos(k_0 L_2) \\ j\sin(k_0 L_2)/Z_0 & \cos(k_0 L_2) \end{pmatrix} \begin{pmatrix} p_3 \\ 0 \end{pmatrix}$$

$$\begin{pmatrix} p_1 \\ U_1 \end{pmatrix} = \begin{pmatrix} \cos(k_0 L_2) + \frac{jZ_A \sin(k_0 L_2)}{Z_0} \\ \frac{j\sin(k_0 L_2)}{Z_0} \end{pmatrix} p_3. \tag{3}$$

Ingard and Dear method uses the ratio between the complex sound pressures at microphone positions 1 and 3, which can be obtained from Eq. (3) as

$$\frac{p_1}{p_3} = \cos(k_0 L_2) + \frac{jZ_A \sin(k_0 L_2)}{Z_0}, \tag{4}$$

and Z_A is given by

$$Z_A = -jZ_0 \left(\frac{p_1}{p_3} \frac{1}{\sin(k_0 L_2)} - \cot(k_0 L_2) \right). \tag{5}$$

For frequencies at which L_2 is precisely an odd number of quarter-wavelengths, the cotangent in Eq. (4) cancels out, and Z_A is given by

$$Z_A = \pm\, jZ_0 \frac{p_1}{p_3}. \tag{6}$$

The normalized flow resistance, θ, is determined from Eq. (6) as the absolute value of the imaginary part of the sound pressure ratio:

$$\theta = \left| \mathrm{Im} \frac{p_1}{p_3} \right|. \tag{7}$$

Thus, the airflow resistance can be determined from Eq. (1) at low frequencies and the airflow resistivity, σ, determined by dividing Eq. (1) by the sample thickness:

$$\sigma = R_s/d. \tag{8}$$

A comparison between the Ingard and Dear method and two other approaches for measuring the airflow resistivity was presented in [19].

2.2. *The proposed electroacoustic method*

Alba et al. [18] developed an electroacoustic method based on the device presented by Dragonetti et al. [17]. The Ingard and Dear device can also be modified using the same rationale. Therefore, the device shown in Fig. 1a is now considered without measuring the sound pressure at the microphone positions. Instead, the total electric impedance is measured directly at the two terminals of the speaker over the frequency range in use.

We note that the rigidly terminated standing wave tubes in Fig. 1 are closed by a loudspeaker. A direct-radiator loudspeaker is an electrodynamic transducer that converts an electric current into a mechanical vibration. It works by the interaction of the electric current passing through a moving coil and the magnetic field of a permanent magnet. The coil is located in the air gap of the magnet, and it is rigidly attached to a diaphragm that serves as the sound radiating element. To establish the electroacoustic method, we must now consider the effect caused by the interaction between the loudspeaker and the mechanical impedance of the acoustic load on its diaphragm.

In an electrodynamic transducer, the total electric impedance, Z_{ET}, of the device in Fig. 1a is given by [25],

$$Z_{ET} = Z_E + Z_{MOT} = Z_E + \frac{(Bl)^2}{Z_{AT} S^2}, \tag{9}$$

where Z_{MOT} is called the motional impedance, Z_E is the pure electric impedance of the loudspeaker given by

$$Z_E = R_E + j\omega L_E, \tag{10}$$

R_E and L_E are, respectively, the electric resistance and inductance of the voice coil, ω is the angular frequency, S is the diaphragm effective area (considered as equal to the cross-sectional area of the tube at low frequencies), Bl is the loudspeaker's force factor, and Z_{AT} is the total acoustic impedance of the system. In this case, Z_{AT} is the mechanical impedance of the acoustic load on the loudspeaker, $Z_{A0}S^2$, plus the effect of the mechanical impedance of the loudspeaker, Z_M, so Eq. (9) is written as:

$$Z_{ET} = Z_E + \frac{(Bl)^2}{Z_M + Z_{A0} S^2}. \tag{11}$$

2.3. Estimating the airflow resistance and reactance

In the electroacoustic method, two measurements are needed to determine the airflow resistance of a sample material: one without and one with the sample material in the tube. The measurement without the sample is used to calibrate the system.

2.3.1. System without the sample

In addition to the values of Z_E and Bl of the loudspeaker, the mechanical impedance of the mechanical elements in the loudspeaker, Z_M, must be known.

This impedance can be obtained in a calibration process by measuring the total electric impedance at the loudspeaker's terminals without the material sample in the tube (see Fig. 1b).

The acoustic impedance of an empty lossless tube of length L_1 and terminated with a rigid end (infinite impedance) is purely reactive, and is given by the equation [1, 25]:

$$Z_{A1} = \frac{p_1}{U_1} = -jZ_0 \cot(k_0 L_1)\,. \tag{12}$$

Taking into account the effect of the loudspeaker, which is mechanically loaded by this empty tube [see Eq. (11)], the total electric impedance at the terminals of the loudspeaker is:

$$Z_{ET} = Z_E + \frac{(Bl)^2}{Z_M - jZ_0 \cot(k_0 L_1)\, S^2}. \tag{13}$$

If the frequency of the sound is selected such that $f_n = \frac{(2n-1)c_0}{4L_1}$, Eq. (13) becomes:

$$Z_{ET} = Z_E + \frac{(Bl)^2}{Z_M}. \tag{14}$$

Note that when the frequency approaches zero (DC), the loudspeaker electric impedance approaches the voice coil resistance asymptotically so that R_E can be determined directly from the impedance curve. At such frequencies, the loudspeaker's electrical reactance, ωL_E, becomes neglectable. There are several possible methods for measuring the value of Bl [25]; however, loudspeaker manufacturers commonly provide this parameter. After the total electrical impedance has been measured without the sample as a function of the frequency, the values of the mechanical impedance, Z_M, can be obtained using Eq. (14). These values will later be used to determine the acoustic impedance of the porous materials.

2.3.2. System with the sample

The tube with the material sample of acoustic impedance Z_A (se Fig. 1a) is described using the transfer matrix method by the following equation,

$$\begin{pmatrix} p_0 \\ U_0 \end{pmatrix} = \begin{pmatrix} \cos(k_0L_1) & jZ_0\sin(k_0L_1) \\ \frac{j\sin(k_0L_1)}{Z_0} & \cos(k_0L_1) \end{pmatrix} \begin{pmatrix} 1 & Z_A \\ 0 & 1 \end{pmatrix} \begin{pmatrix} \cos(k_0L_2) & jZ_0\sin(k_0L_2) \\ \frac{j\sin(k_0L_2)}{Z_0} & \cos(k_0L_2) \end{pmatrix} \begin{pmatrix} p_3 \\ U_3 \end{pmatrix}, \tag{15}$$

and the acoustic impedance, Z_{A0}, is obtained as

$$Z_{A0} = \frac{p_0}{U_0} = -jZ_0 \frac{\cos\left(k_0(L_1+L_2)\right) + j\frac{Z_A}{Z_0}\cos\left(k_0L_1\right)\sin\left(k_0L_2\right)}{\sin\left(k_0\left(L_1+L_2\right)\right) + j\frac{Z_A}{Z_0}\sin\left(k_0L_1\right)\sin\left(k_0L_2\right)}. \tag{16}$$

If the frequency of the sound is selected to be the same as in the calibration process, $f_n = \frac{(2n-1)c_0}{4L_1}$, then $\cos(k_0L_1) = 0$ and $\sin(k_0L_1) = \pm 1$, and Eq. (16) is written as

$$Z_{A0} = -jZ_0 \frac{\pm\sin\left(k_0L_2\right)}{\pm\cos\left(k_0L_2\right) \pm j\frac{Z_A}{Z_0}\sin\left(k_0L_2\right)} = \frac{Z_0}{j\cot\left(k_0L_2\right) - \frac{Z_A}{Z_0}}. \tag{17}$$

Now, if $L_1 = L_2$, Eq. (17) is simplified to

$$Z_{A0} = -\frac{Z_0^2}{Z_A}. \tag{18}$$

By substituting Eq. (18) into Eq. (11), we get

$$Z_{ET} = Z_E + \frac{(Bl)^2}{Z_M - \frac{Z_0^2}{Z_A}S^2}. \tag{19}$$

In Eq. (19), we may identify the term $-(Z_0S)^2/Z_A$ as a material mechanical impedance, denoted here as Z_{m0}. We can now solve Eq. (19) for Z_A using the value of Z_M obtained during the calibration process, the measured values of Z_{ET} and Z_E, and the value of Bl provided by the loudspeaker manufacturer. The specific airflow resistance corresponds to the real part of Z_A for those frequencies chosen in the same way as in the Ingard and Dear method. Finally, the airflow resistivity of the material is obtained from Eq. (8).

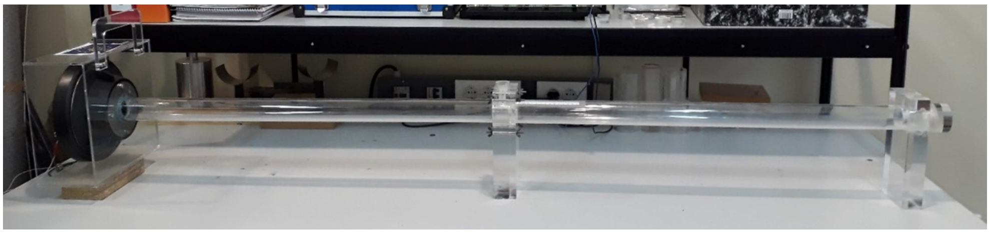

Figure 2: Custom-made experimental device to implement the electroacoustic method.

3. Materials and method

An experimental setup based on the Ingard and Dear device was built to implement the method described in the previous section (see Fig. 2). The device was made of a 5 mm-thick polymethylmethacrylate (PMMA) cylindrical tube with an inner diameter of 42 mm. The cut-off frequency for this diameter is around 4800 Hz. The standing wave tube entrance was closed with an electrodynamic loudspeaker (Beyma CP-800Ti). An adjustable 25 mm-thick acoustically rigid termination was used to close the tube end. The perforations used to insert the two microphones in the Ingard and Dear method were sealed. Other parts of the device were also carefully sealed to avoid the effects of air leaks on the results. After the test sample was placed, the tube was divided into two equal sections of length $L_1 = L_2 = 89.1$ cm by adjustment of the rigid termination.

A 100 Ω reference resistor was connected in series between the variable frequency sine wave generator and the loudspeaker. The impedance magnitude and phase were estimated by measuring the voltage across the reference resistor and the loudspeaker connection terminals. The results were obtained using computer-based loudspeaker impedance measurement software (LIMP from Artalabs [26]) running on a USB-connected laptop with a Behringer UMC202HD audio interface set to 48 kHz sampling rate and 24-bit resolution. The system's

SNR, according to manufacturer specs, is 100 dB. The two audio interface channels were calibrated before each data set to reduce the error caused by potential channel level differences and ensure less than 0.1 dB of difference between them. The software uses the remaining difference after calibration to determine the gain that will be applied to each channel when measuring the impedance.

To ensure a high measurement signal/noise ratio, a stepped sine wave signal with 1/48 octave increments covering a frequency range from 5 to 1000 Hz was used to excite the system. The equations for determining the airflow resistivity that were outlined in Section 2.3 were implemented into Matlab codes to calculate the results. The tests were conducted at room temperature, and $\rho_0 = 1.18$ kg/m^3, and $c_0 = 345$ m/s were considered during the experiments.

Six different porous materials with different thicknesses and bulk densities ranging between 8.7 and 130.2 kg/m^3 were used to test the electroacoustic method. They included four samples of foam and two fibrous materials commercially available for sound absorption applications, and represented a wide range of airflow resistivity values. Table 1 presents the thickness and bulk density values, and Fig. 3 shows photographs of each material. Note that the samples tagged as AFM1, AFM2, and TFB are recycled materials.

The recommendations given in the ISO standards for the determination of airflow resistance were carefully followed for the preparation and fitting of the samples [6, 7]. Measurement of airflow resistivity was carried out on three different samples of each material, and their arithmetic mean was recorded. In addition, three sets of measurements were performed on different days to test the repeatability of the experimental results. To minimize possible effects of the samples' internal structural characteristics, they were tagged after the first test to repeat all the measurements in the same orientation.

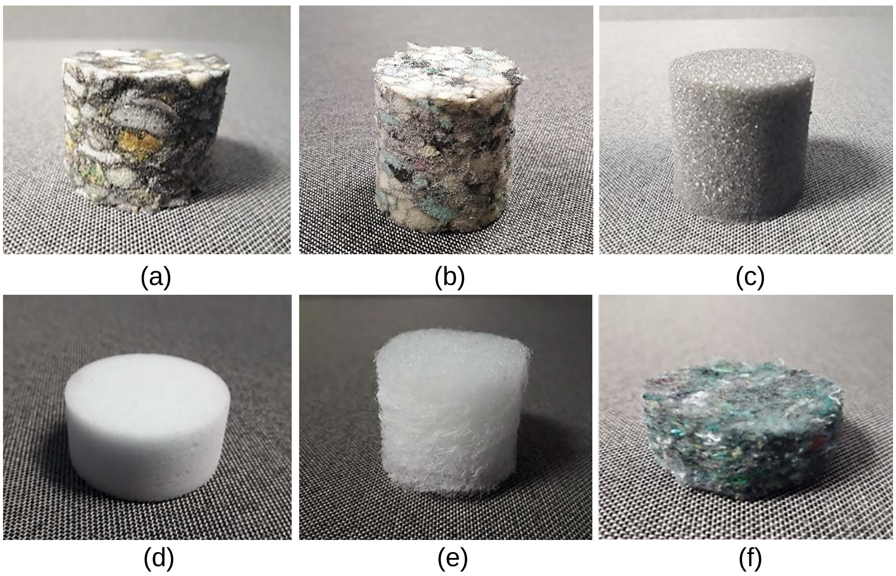

Figure 3: Photographs of the material samples used in the experiments: (a) Agglomerated polyurethane foam (AFM1); (b) Agglomerated polyurethane foam (AFM2); (c) Polyurethane foam (PFM); (d) Melamine foam (MFM); (e) Polyester fibers (PFB); (f) Textile fibers (TFB).

Table 1: Thickness and bulk density of the material samples used in the experiments.

Material	Thickness (mm)	Density (kg/m^3)
Agglomerated Polyurethane Foam (AFM1)	30	130.2 ± 2.0
Agglomerated Polyurethane Foam (AFM2)	40	83.3 ± 2.0
Polyurethane Foam (PFM)	40	22.2 ± 0.3
Melamine Foam (MFM)	20	8.7 ± 0.1
Polyester Fibers (PFB)	36	15.4 ± 0.1
Textile Fibers (TFB)	14	54.1 ± 4.4

4. Results

As described in the theoretical section, a calibration process is required to determine the loudspeaker mechanical impedance by measuring the total electric impedance with the empty tube. The measurement should be carried out at those excitation frequencies at which the length of the tube is precisely an odd number of quarter-wavelengths. Since $L_1 = 89.1$ cm, these theoretical frequencies are 96.8, 290.4, 484.0, 676.6 Hz, etc.

Figure 4 shows the results of the total electric resistance and reactance measured at the loudspeaker terminals as a function of the frequency.

The loudspeaker's mechanical impedance, Z_M, is obtained from Eq. (14) using the previously measured values of Z_E, ($R_E = 5.52$ ohms and $L_E = 0.13$ mH), $Bl = 15$ N/A (given by the loudspeaker's manufacturer), and the measured results of Z_{ET} as shown in Fig. 4. Figure 5 shows the resulting loudspeaker's mechanical impedance when there is no sample in the tube.

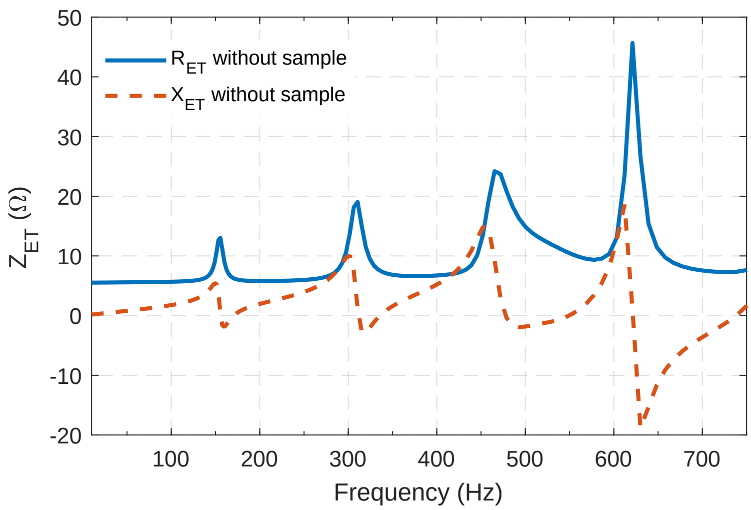

Figure 4: Total electric impedance (Z_{ET}) measured during the calibration process when there is no sample in the tube.

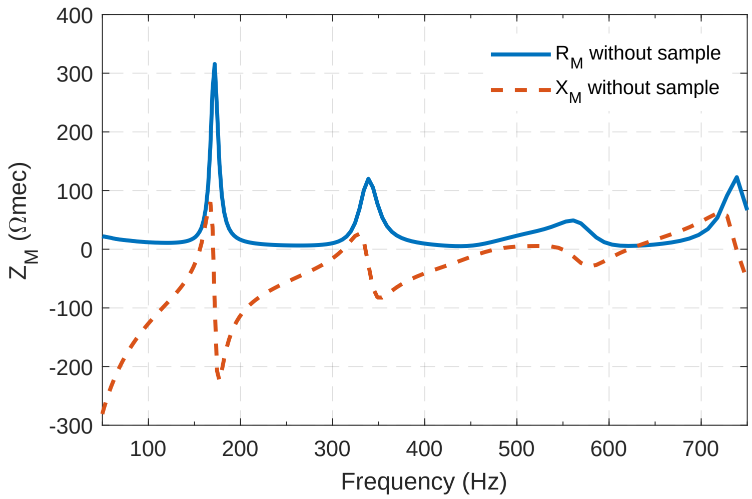

Figure 5: Loudspeaker mechanical impedance (Z_M) determined during the calibration process when there is no sample in the tube.

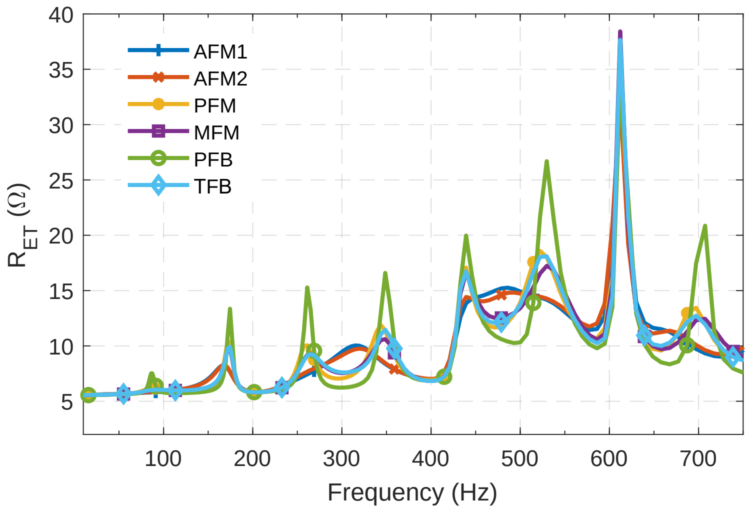

Figure 6: Total electric resistance measured at the loudspeaker terminals (R_{ET}) with different sample materials inserted in the tube.

4.1. Airflow resistance measurement

After the system had been calibrated, the total electric impedance at the loudspeaker terminals was measured with the sample material of thickness d, placed inside a tube of length $L_1 + L_2 + d$. The measured results of the total electric resistance and reactance are presented in Figs. 6 and 7, respectively.

The effects caused by the acoustic resistance provided by the different porous materials, both in magnitude and in the frequency of the peaks, are observed in the electric impedance curves. The corresponding plots for the material mechanical resistance (R_{m0}) and reactance (X_{m0}) are shown in Figs. 8 and 9, respectively.

The differences between the curves of the total electric and the total mechanical resistance are better appreciated by focusing on the neighborhood of the first frequency at which L_1 is precisely an odd number of quarter-wavelengths (f_1 = 96.8 Hz). These values are shown in Figs. 10 and 11, respectively, to offer

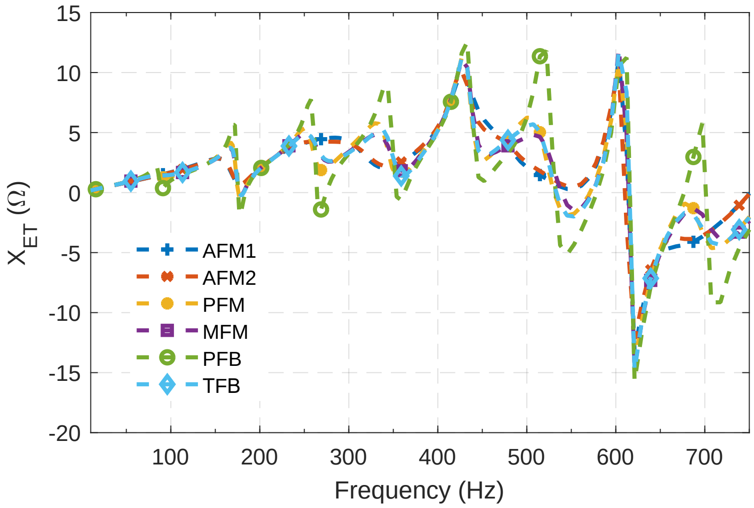

Figure 7: Total electric reactance measured at the loudspeaker terminals (X_{ET}) with different sample materials inserted in the tube.

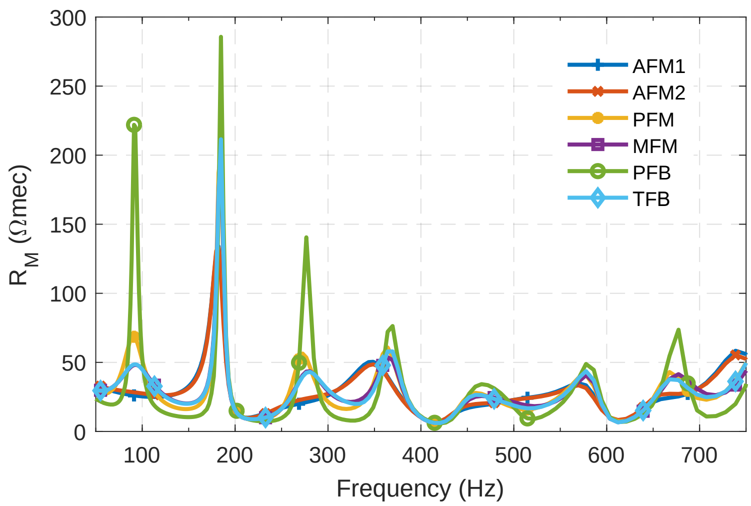

Figure 8: Mechanical resistance (R_{m0}) determined from Eq. (19) with different sample materials inserted in the tube.

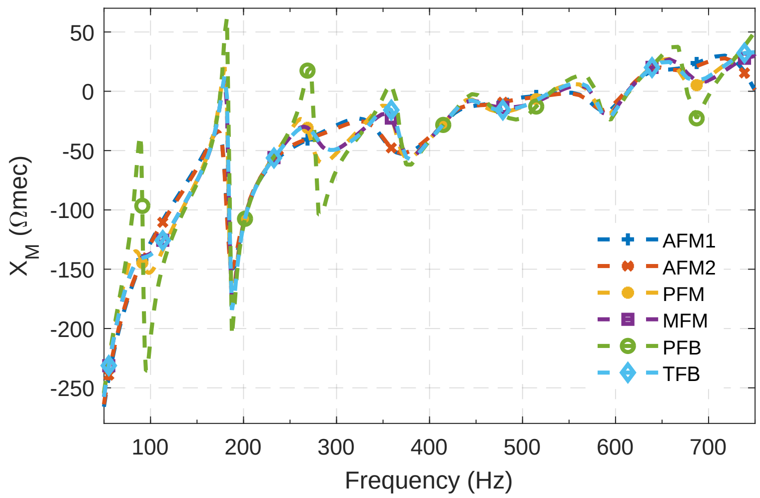

Figure 9: Mechanical reactance (X_{m0}) determined from Eq. (19) with different sample materials inserted in the tube.

more insight into measured data. At that frequency, we note that the highest value of mechanical resistance is obtained for the material made of polyester fibers (PFB), while the lowest value is obtained for the agglomerated polyurethane foam of the highest bulk density (AFM1).

Since, at low frequencies, the acoustic impedance in the material is inversely proportional to the mechanical impedance [see Eq. (19)], it was expected that the highest value of airflow resistance would be obtained for the material denoted as AFM1. In contrast, the lowest value would correspond to the material made of polyester fibers (PFB).

The specific airflow resistance of each material was determined as the real part of their acoustic impedances obtained by Eq. (19). The three tests carried out for each material, and their average results, are presented in Table 2. The average results were calculated using the individual results of all the samples for each material, combining the results of the three tests. The small differences

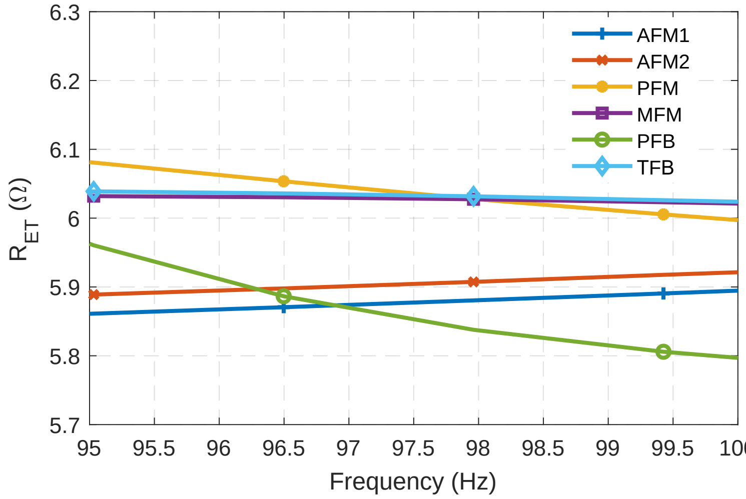

Figure 10: Zoom-in of Fig. 6 to show the total electric resistance (R_{ET}) in the neighborhood of f_1 = 96.8 Hz in detail.

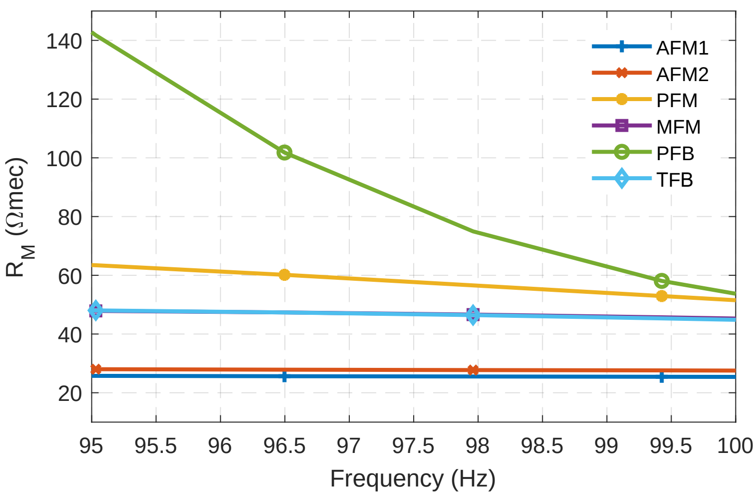

Figure 11: Zoom-in of Fig. 6 to show the total electric resistance (R_{m0}) in the neighborhood of f_1 = 96.8 Hz in detail.

observed in the results of tests may have been caused by several factors, such as slight material inhomogeneities, the fitting of the samples, and minor changes in room temperature.

Table 2: Average results of airflow resistance for each material sample obtained in the experimental tests.

	Airflow resistance, R_s (Ns/m^3)			
Material	Test 1	Test 2	Test 3	Mean
AFM1	800.9 ± 25.9	778.0 ± 30.5	769.9 ± 16.5	782.9 ± 24.3
AFM2	686.9 ± 29.9	662.8 ± 32.6	748.2 ± 37.5	699.3 ± 45.2
PFM	191.0 ± 6.5	193.0 ± 2.5	177.2 ± 2.4	187.1 ± 7.9
MFM	300.2 ± 2.6	294.1 ± 1.5	284.6 ± 1.7	293.0 ± 6.6
PFB	45.3 ± 0.2	52.3 ± 0.2	44.43 ± 0.4	47.3 ± 3.5
TFB	294.7 ± 48.1	301.9 ± 45.9	299.2 ± 47.4	298.6 ± 38.6

Subsequently, the values of airflow resistivity for each material were determined by dividing their resistance by the sample thicknesses [see Eq. (8)]. It is worth mentioning that the thicknesses of all the samples were very small compared to the approximate wavelength of 3.7 m, at which the results of airflow resistance were estimated. For such a large wavelength, and assuming that $kd = 0.2$ is small enough to satisfy the theory, a maximum material thickness of about 11 cm would be measurable in the device.

The samples were also measured using the Ingard and Dear method to assess the validity of the results obtained with the proposed method. These measurements were made with the same setup, but now sound pressures were measured at the front faces of the samples and the front of the reflecting termination using two high-precision 1/2-inch microphones and built-in preamplifiers (Bruel

& Kjaer Type 4190-L-001). The microphone signals were previously calibrated (Bruel & Kjaer Type 4231) and processed by a multichannel digital signal analyzer (Bruel & Kjaer PULSE). Care was taken to measure the samples in the same orientation as that used in the proposed method. Additionally, the airflow resistivity of the samples was measured using the static airflow method described in ISO 9053-1 [6]. The material labeled as PFB has a too small resistivity and could not be possible to measure such a low-pressure drop across the test specimen with the equipment available.

Table 3 shows the comparison between the results obtained by all methods. We can see reasonably good agreement between the results.

Table 3: Average airflow resistance and resistivity results for each material sample, obtained using the Ingard and Dear method [10], the ISO 9053-1 method [6], and the proposed electroacoustic method.

	Airflow resistance, R_s (Ns/m^3)		Airflow resistivity, σ (kNs/m^4)		
Material	Proposed method	Ingard and Dear method	Proposed method	Ingard and Dear method	ISO 9053-1 method
AFM1	782.9 ± 24.3	785.0 ± 0.1	26.1 ± 0.8	26.2 ± 0.1	27.0 ± 2.1
AFM2	699.3 ± 45.2	704.9 ± 26.7	17.5 ± 1.1	17.6 ± 0.7	17.0 ± 1.3
PFM	187.1 ± 7.9	181.5 ± 6.8	4.7 ± 0.2	4.5 ± 0.2	5.0 ± 0.7
MFM	293.0 ± 6.6	291.8 ± 2.2	14.6 ± 0.3	14.6 ± 0.1	18.3 ± 2.1
PFB	47.3 ± 3.5	43.3 ± 1.2	1.3 ± 0.1	1.2 ± 0.1	–
TFB	298.6 ± 38.6	310.6 ± 53.6	21.3 ± 2.8	22.2 ± 3.8	23.0 ± 4.1

We note that the most significant errors of the approach presented here concerning the method of Ingard and Dear occurred in the use of samples of fibrous materials (polyester and textile waste fibers). These samples exhibited relative error values between 4.0 and 8.3%. This fact may be related to the inhomogeneity typical of these materials and inherent differences in the cutting and fitting of the samples in the tube. The results were much better in the case of foams, where the relative error of the new method did not exceed 4.4%. It is noted that several sources of uncertainty may affect the measurement method, including electrical impedances, environmental values, sample geometrical measurements, and loudspeaker's force factor. An uncertainty analysis is shown in the appendix.

5. Conclusions

This paper presented an electroacoustic method for indirectly measuring the airflow resistivity of porous materials. The method follows the ideas for an alternative method presented previously by the authors [18], which has now been applied to the standing wave tube described by Ingard and Dear. The airflow resistivity is determined by directly measuring the electric impedance at the loudspeaker's terminals after a simple calibration process. In this study, the airflow resistivity of several porous materials with a wide range of airflow resistivity values was measured to validate the approach. Results were compared with those obtained through the Ingard and Dear method and the ISO 9053-1 standard.

It was observed that the results of the proposed method are in reasonable agreement with the results using the ISO standard and the Ingard and Dear methodology, even though the new method seems more accurate for foams than for inhomogeneous fibrous samples. Moreover, previous work has indicated that the method developed by Ingard and Dear gives results comparable to those of the ISO standardized method [19]. Thus, the proposed approach could be a potential alternative to conventional methods.

Although it is simple and inexpensive to build, the experimental device may be bulky compared to other setups. However, after a straightforward calibration of the device, an obvious advantage of the method presented in this paper is that using microphones to measure sound pressure is unnecessary. In addition, the use of complex measurement instrumentation is not required. For these reasons, this method enables a low-cost process of estimating airflow resistivity in porous materials with an acceptable degree of accuracy.

Acknowledgments

This work has been financially supported by the Conselleria de Innovacion, Universidades, Ciencia y Sociedad – Generalitat Valenciana, through the ACIF-2020 program [grant number ACIF/2020/401], and the European Social Fund.

CRediT author statement

JC Rodríguez: Conceptualization, Data curation, Formal analysis, Methodology, Software, Visualization, Writing - original draft, Writing - review & editing. **J Alba:** Conceptualization, Formal analysis, Methodology, Software, Supervision, Project administration. **JP Arenas:** Conceptualization, Data curation, Visualization, Writing - original draft, Writing - review & editing. **R del Rey:** Conceptualization, Methodology, Software, Supervision, Project administration.

References

[1] Allard JF, Atalla N. Propagation of sound in porous media: Modelling sound absorbing materials. 2nd ed. Chichester: Wiley; 2009.

[2] Bies DA, Hansen CH. Flow resistance information for acoustical design. Appl Acoust 1980;13:357391. https://doi.org/10.1016/0003-682x(80)90002-x

[3] Garai M, Pompoli F. A simple empirical model of polyester fibre materials for acoustical applications. Appl Acoust 2005;66:13831398. https://doi.org/10.1016/j.apacoust.2005.04.008

[4] Bonfiglio P, Pompoli F. Inversion problems for determining physical parameters of porous materials: overview and comparison between different methods. Acta Acustica united with Acustica 2013;99:341351. https://doi.org/10.3813/aaa.918616

[5] Berardi U, Iannace, G. Predicting the sound absorption of natural materials: Best-fit inverse laws for the acoustic impedance and the propagation constant. Appl Acoust 2017;115:131138. https://doi.org/10.1016/j.apacoust.2016.08.012

[6] ISO 9053-1:2018. Acoustics Determination of airflow resistance Part 1: Static airflow method, Geneva, Switzerland; 2018.

[7] ISO 9053-2:2020. Acoustics Determination of airflow resistance Part 2: Alternating airflow method. Geneva, Switzerland; 2020.

[8] ASTM C522-03. Standard Test Method for Airflow Resistance of Acoustical Materials, West Conshohocken, PA; 2016.

[9] Stinson MR, Daigle GA. Electronic system for the measurement of flow resistance. J Acoust Soc Am 1988;83:24222428. https://doi.org/10.1121/1.396321

[10] Ingard KU, Dear TA. Measurement of acoustic flow resistance. J Sound Vib 1985;103:567572. https://doi.org/10.1016/S0022-460X(85)80024-9

[11] Woodcock R, Hodgson M. Acoustic methods for determining the effective flow resistivity of fibrous materials. J Sound Vib 1992;153:186191. http://dx.doi.org/10.1016/0022-460x(92)90639-F

[12] Ren M, Jacobsen F. A method of measuring the dynamic flow resistance and reactance of porous materials. Appl Acoust 1993;39:265276. https://doi.org/10.1016/0003-682x(93)90010-4

[13] Picard MA, Solana P, Urchuegua JF. A method of measuring the dynamic flow resistance and the acoustic measurement of the effective static flow resistance in stratified rockwool samples. J Sound Vib 1998;216:495505. https://doi.org/10.1006/jsvi.1998.1725

[14] Sebaa N, Fellah ZEA, Fellah M, Lauriks W, Depollier C. Measuring flow resistivity of porous material via acoustic reflected waves. J Appl Phys 2005;98:084901. https://doi.org/10.1063/1.2099510

[15] Panneton R, Olny X. Acoustical determination of the parameters governing viscous dissipation in porous media. J Acoust Soc Am 2006;119:20272040. https://doi.org/10.1121/1.2169923

[16] Doutres O, Salissou Y, Atalla N, Panneton R. Evaluation of the acoustic and non-acoustic properties of sound absorbing materials using a three-microphone impedance tube. Appl Acoust 2010;71:506509. https://doi.org/10.1016/j.apacoust.2010.01.007

[17] Dragonetti R, Ianniello C, Romano RA. Measurement of the resistivity of porous materials with an alternating air-flow method. J Acoust Soc Am 2011;129:753764. https://doi.org/10.1121/1.3523433

[18] Alba J, Arenas JP, del Rey R, Rodrguez JC. An electroacoustic method for measuring airflow resistivity of porous sound-absorbing materials. Appl Acoust 2019;150:132137. https://doi.org/10.1016/j.apacoust.2019.02.009

[19] del Rey R, Alba J, Arenas JP, Ramis J. Evaluation of two alternative procedures for measuring airflow resistance of sound absorbing materials. Arch Acoust 2013;38:547554. https://doi.org/10.2478/aoa-2013-0064

[20] Garai M, Pompoli F. A European inter-laboratory test of airflow resistivity measurements. Acta Acustica united with Acustica 2003;89:471478.

[21] Delany ME, Bazley EN. Acoustic properties of fibrous absorbent materials. Appl Acoust 1971;3:105-116. https://doi.org/10.1016/0003-682X(70)90031-9

[22] Tao JC, Wang P, Qiu XJ, Pan J. Static flow resistivity measurements based on the iso 10534.2 standard impedance tube. Build Environ 2015;94:853-858. http://dx.doi.org/10.1016/j.buildenv.2015.06.001

[23] Doutres O, Salissou Y, Atalla N, Panneton R. Evaluation of the acoustic and non-acoustic properties of sound absorbing materials using a three-microphone impedance tube. Appl Acoust 2010;71:506-509. http://dx.doi.org/10.1016/j.apacoust.2010.01.007

[24] Alba J, Arenas JP, del Rey R, Rodriguez JC. Electroacoustic method for measuring air-flow resistivity in a standing wave tube. Proc. Internoise 2019, June 16-19, Madrid; 2019.

[25] Beranek L, Mellow T. Acoustics: sound fields, transducers and vibration, 2nd ed. London: Academic Press; 2019.

[26] Mateljan I. LIMP - Program for loudspeaker impedance measurement, User manual. ver. 1.9.4, Artalabs, Kastel Luksic, Croatia; 2021.

Appendix

In the proposed method, the following equation is used for the calibration process:

$$Z_{ET} = Z_E + \frac{(Bl)^2}{Z_M}. \tag{20}$$

and the measurement with the sample in the tube uses the equation

$$Z'_{ET} = Z_E + \frac{(Bl)^2}{Z_M - \frac{Z_0^2}{Z_A}S^2} = Z_E + \frac{(Bl)^2}{Z_M + Z_{m0}}. \tag{21}$$

Combining Eqs. (20) and (21), Z_A is determined as a function of the measured data as

$$Z_A = \left(\frac{Z_0 S}{Bl}\right)^2 \frac{Z_{ET} - Z'_{ET}}{(Z'_{ET} - Z_E)(Z_{ET} - Z_E)}. \tag{22}$$

By substituting $K_1 = (Z_0 S/Bl)^2$, $K_2 = Z_{ET} - Z'_{ET}$, $K_3 = Z'_{ET} - Z_E$, and $K_4 = Z_{ET} - Z_E$ into Eq. (22), we get

$$Z_A = \frac{K_1 K_2}{K_3 K_4}. \tag{23}$$

Taking partial derivatives with respect to Z_0, S, Bl, Z_{ET}, Z'_{ET}, and Z_E of K_1, K_2, K_3, and K_4, we obtain

$$|\partial K_1| = 2Z_0 \left(\frac{S}{Bl}\right)^2 |\partial Z_0| + 2S \left(\frac{Z_0}{Bl}\right)^2 |\partial S| + 2\frac{(Z_0 S)^2}{(Bl)^3} |\partial (Bl)|, \tag{24}$$

$$|\partial K_2| = |\partial Z'_{ET}| + |\partial Z_{ET}|, \tag{25}$$

$$|\partial K_3| = |\partial Z'_{ET}| + |\partial Z_E|, \tag{26}$$

$$|\partial K_4| = |\partial Z_{ET}| + |\partial Z_E|. \tag{27}$$

Now, taking partial derivatives with respect to K_1, K_2, K_3, and K_4 of Eq. (23), yields

$$|\partial Z_A| = \frac{K_2}{K_3 K_4}|\partial K_1| + \frac{K_1}{K_3 K_4}|\partial K_2| + \frac{K_1 K_2}{(K_3)^2 K_4}|\partial K_3| + \frac{K_1 K_2}{K_3 (K_4)^2}|\partial K_4|. \tag{28}$$

Since the real part of $|\partial Z_A|$ is $|\partial R_s|$, the uncertainty of the airflow resistivity measurement, $\sigma = R_s/d$, can be obtained by

$$|\partial\sigma| = \frac{|\partial R_s|}{d} + \frac{R_s|\partial d|}{d^2}. \tag{29}$$